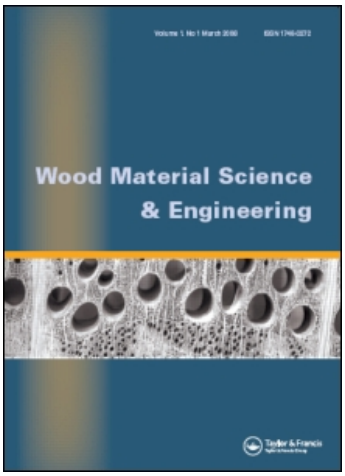

Wood Material Science and Engineering
Publication details, including instructions for authors and subscription information:
http://www.informaworld.com/smpp/title~content=t741771155

Relationship between wood porosity, wood density and methyl methacrylate impregnation rate

Wei-Dan Ding [ab]; Ahmed Koubaa [ab]; Abdelkader Chaala [c]; Tikou Belem [b]; Cornelia Krause [d]
[a] Chaire de recherche du Canada sur la valorisation, la caractérisation et la transformation du bois, [b] Department of Applied Sciences, Université du Québec en Abitibi-Témiscamingue, Rouyn-Noranda, Québec, Canada [c] Service de Recherche et d'expertise en Transformation des produits forestiers (SEREX), Amqui, Québec, Canada [d] Department of Fundamental Sciences, Université du Québec à Chicoutimi, Chicoutimi, Québec, Canada

Online Publication Date: 01 March 2008

To cite this Article Ding, Wei-Dan, Koubaa, Ahmed, Chaala, Abdelkader, Belem, Tikou and Krause, Cornelia(2008)'Relationship between wood porosity, wood density and methyl methacrylate impregnation rate',Wood Material Science and Engineering,3:1,62 — 70

To link to this Article: DOI: 10.1080/17480270802607947

URL: http://dx.doi.org/10.1080/17480270802607947

Wood Material Science and Engineering, 2008; 1–2: 62–70

Taylor & Francis
Taylor & Francis Group

ORIGINAL ARTICLE

Relationship between wood porosity, wood density and methyl methacrylate impregnation rate

WEI-DAN DING[1,2], AHMED KOUBAA[1,2], ABDELKADER CHAALA[3], TIKOU BELEM[2] & CORNELIA KRAUSE[4]

[1]*Chaire de recherche du Canada sur la valorisation, la caractérisation et la transformation du bois,* [2]*Department of Applied Sciences, Université du Québec en Abitibi-Témiscamingue, Rouyn-Noranda, Québec, Canada,* [3]*Service de Recherche et d'expertise en Transformation des produits forestiers (SEREX), Amqui, Québec, Canada, and* [4]*Department of Fundamental Sciences, Université du Québec à Chicoutimi, Chicoutimi, Québec, Canada*

Abstract
Mercury intrusion porosimetry (MIP) was used to evaluate the impregnation mechanisms of wood by methyl methacrylate (MMA) through examining the changes in porosity, pore volume, pore size distribution and bulk density of solid wood before and after MMA impregnation. Porosities of MMA-impregnated (hardened) wood samples were lower than those of solid wood samples for six studied species, five hardwoods and one softwood. Densities of hardened wood were enhanced from 45 to 130% depending on the species. The pore volume available for mercury intrusion was shifted from pore $d > 0.1$ μm for solid wood to pore $d \leq 0.1$ μm for hardened wood. A pore diameter of 0.1 μm was used as the transition point for MMA impregnation and the increased mercury penetration below this point was attributed to the MMA polymer pore structure. Porosity as an intrinsic property of wood appears to be the main determinant of impregnation rate and polymer retention, especially for porosity with pore diameter > 0.1 μm. The results indicate that the MIP technique is an effective tool with which to study the impregnation process.

Keywords: *Density, hardened wood, impregnation, mercury intrusion porosimetry, pore size distribution, porosity.*

Introduction

Since wood is a heterogeneous biomaterial which is easily subject to dimensional changes, environmental and biological attacks, its durability and mechanical strength are not sufficient for long-term end uses. Therefore, researchers have developed various methods to offset these disadvantages. Impregnation of solid wood has been one of the most discussed techniques in the past decade. The wood, including both hardwood and softwood, has been impregnated by many chemicals such as thermosetting resin (epoxy resin, phenol formaldehyde, urea formaldehyde, etc.) or polymeric monomer (methacrylate, acrylates, styrene, unsaturated polyester, etc.), followed by *in situ* polymerization by radiation or catalyst–thermal treatment (El-Awady, 1999; Solpan & Güven, 1999*a*, b, 2000, 2001; Zhang et al., 2006). To achieve adequate physical, mechanical and antibiological properties, the chemicals must have impregnated into the wood pores before it is cured. Types and conditions of wood are undoubtedly essential for the degree of impregnation, along with the properties of chemicals and impregnation conditions (Solpan & Güven, 1999*a*; Wang & Yan, 2005).

Wood is a porous material, and its pore structure affects its behaviour more than any other characteristics. Knowledge of the pore structure is directly related to the density, permeability, stability, strength, thermal and dielectric properties as well as growth characteristics of wood. Pore geometry and porosity affect several commercial processes, including wood drying, chemical treatment, pulping and bleaching (Stayton & Hart, 1965; Hill & Papadopoulos, 2001; Forsström, 2004).

Correspondence: A. Koubaa, Chaire de recherche du Canada sur la valorisation, la caractérisation et la transformation du bois, Université du Québec en Abitibi-Témiscamingue, 445 BD de l'Université, Rouyn-Noranda, QC, Canada, J9X5E4. E-mail: ahmed.koubaa@uqat.ca

(Received 22 September 2008; accepted 3 November 2008)

ISSN 1748-0272 print/ISSN 1748-0280 online
DOI: 10.1080/17480270802607947

The anatomical structure of wood varies among species. In general, wood can be divided into two classes: hardwood and softwood. Hardwood has a relatively complex structure comprising four main cell types, namely vessels, fibres, ray parenchyma and axial parenchyma, at 20–60%, 15–60%, 5–30% and 1–24% of the volume, respectively (Ona et al., 1999; Almerida & Hernández, 2007). Softwood consists of axial tracheid cells, ray parenchyma and resin canals (for some species), with tracheids as the main component, making up 90–95% of the wood volume (Andersson, 2006). These component cells vary widely in size, ranging from vessels up to or larger than 300 μm in diameter, to cell-wall pits with a radius of 1.0–0.1 μm, to cell-wall cavities as small as 1.5 nm (Stone, 1964; Almerida & Hernández, 2007). Wood microstructures and porosities vary widely accordingly.

Although wood cell dimensions (opening radii) differ, wood pores can be classified into three groups: perforated, semi-open and isolated (Stone, 1964). These three types of pores are schematically illustrated in Figure 1 (before and after mercury intrusion, and after extrusion). Before intrusion, pores are perforated and continuous (Figure 1a–c), with an 'ink-bottle' shape (Figure 1b). Examples of perforated pores are two-end open cutting cells, porous middle lamella with less porous secondary walls on each side and fibres connected laterally via pits. Pores belonging to the semi-open group (Figure 1d–f) are closed-end pores. They include single fibres with pits as openings, aspirated pits and one-ended open cutting fibres. Isolated pores (Figure 1g) are connected to neither interior nor exterior surfaces, and therefore do not contribute to the volume filled by mercury. These voids are caused by cell-wall collapse in oven-dried wood.

Various techniques have been used to determine the wood pore properties, including measuring scanning electron microscopy (SEM), gas adsorption isotherms, determining solute exclusion, thermoporosimetry, nuclear magnetic resonance, small-angle X-ray scattering (SAXS) and mercury intrusion porosimetry (MIP) (Stayton & Hart, 1965; Trenard, 1980; Schneider, 1983; Jakob et al., 1996; Hill & Papadopoulos, 2001; Zhang et al., 2006; Almeida & Hernández, 2007). All have limitations in terms of accessibility to internal pore structure, pore size range of application and physical distortion of the pore structure during analysis. MIP is commonly used to determine the characteristics of porous media owing to its operational ease, rapidity and reproducibility. MIP obtains pore size distributions based on Washburn's theory that a non-wetting liquid (e.g. mercury), which typically has a greater than 90° contact angle with material, cannot spontaneously enter the pore because of surface tension force (Stayton & Hart, 1965; Hill & Papadopoulos, 2001). However, this force may be overcome by external pressure, and the relationship between the applied pressure and the equivalent pore diameter (d) is determined using Washburn's equation (1921):

$$d = \frac{-4\gamma\cos\theta}{P} \tag{1}$$

where P is the applied pressure (Pa), d is the pore diameter (m), γ is the surface tension (N m^{-1}), and θ is the contact angle between wood and mercury (degrees). The commonly accepted surface tension value 0.484–0.473 N m^{-1} has been reported to have a negligible effect on pore diameter determination (Penumadu & Dean, 2000). Contact angles in previous studies have varied from 130 to 140°, depending on several factors such as solid surface structure and mercury purity (Stayton & Hart, 1965; Schneider, 1983; Moura et al., 2005; Almeida & Hernández, 2007).

MIP test results must be interpreted with caution (Roels et al., 2001). First, this method does not measure actual pore size distribution, but rather pore entrance size. For instance, ink-bottle pores (Figure 1b) are characterized not by the size of the bottle, but by the size of the neck. This leads to overestimation of fine pore volume and underestimation of large pore volume (Delage & Lefebvre, 1984; Roels et al., 2001). Secondly, Washburn's equation assumes pores of a circular cross-section, although in reality, it is somewhat closer to real pore shape. Thus, Cook and Hover (1993) suggest that a shape factor should be incorporated into eq. (1). Thirdly, the particularly high pressure used in the test inevitably leads to compression of specimens, and consequently the collapse of a number of pores or voids (Stone, 1964; Hill & Papadopoulos, 2001).

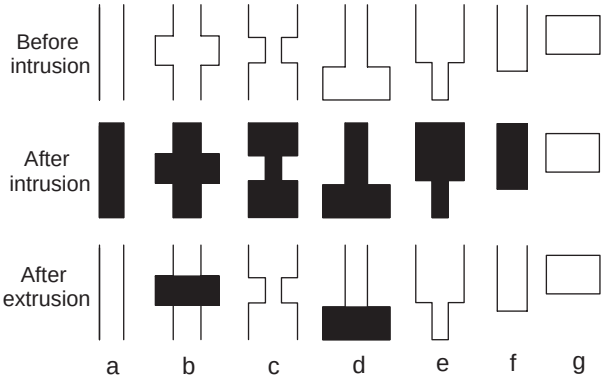

Figure 1. Schematic illustration of wood pore types and their states after mercury intrusion and extrusion. (All drawings assume that openings are connected to the surface.)

The isolated spaces produced could influence the measured porosity. Finally, when applying MIP to wood, the anisotropic characteristics of this material must be taken into account, particularly in the longitudinal direction (Almeida & Hernández, 2007).

Despite its limitations, MIP is effective in assessing the responses of wood to several processes and phenomena. Almeida and Hernández (2007) applied MIP to seven hardwoods using a 3 mm section cut in the longitudinal direction to detect pore structure and illustrated the effect of pore structure on moisture desorption under different relative humidity conditions. This method was also used to evaluate the pore structure of sheets of paper (Moura et al., 2005). Stayton and Hart (1965) used MIP
to determine pore size distributions and cell-wall densities of three softwood species using thin samples 320 μm thick. Trenard (1980) compared pore volumes and pore size distributions of beech, spruce, Scots pine and fir using MIP and investigated the effect of axial length (240 μm, 320 μm and 10 mm) on mercury penetration. MIP was also used to evaluate the impregnability of several hardwoods and softwoods (22 mm axial length), and mercury penetration was found to be comparable to wood impregnation by a creosote preservative (Schneider, 1983). Wang and Yan (2005) used MIP at 138 MPa intrusion pressure to characterize phenol formaldehyde resin penetration in birch and aspen veneer under different curing conditions. Liquid resin penetrated mainly into the large pores ($\geq$40 μm for birch and $\geq$10 μm for aspen) for specimens cured in an oven. However, smaller pores (1 μm $< d <$ 3 μm for birch and $d <$ 0.5 μm for aspen) were filled under hot-press curing conditions.

Although many studies have focused on the pore structures of wood, the mechanisms of polymeric monomer impregnation in solid wood to form hardened wood are still unclear. The relationships between porosity and impregnation rate, porosity and polymer retention, and location of the polymer are still in question. Therefore, the objective of this study is to evaluate the effects of wood porosity and pore structure, measured using MIP, on the methyl methacrylate (MMA) impregnation process.

Materials and methods

Materials

Five hardwoods: hybrid poplar (*Populus* ×*euramericana*), aspen (*Populus tremuloides* Michx), white ash (*Fraxinus rubra*), red oak (*Quercus alba*) and silver maple (*Acer saccharinum*); and one softwood: northern white cedar (*Thuja occidentalis*), were obtained from various suppliers. Specimens were randomly selected from different boards. The five hardwoods fall into two groups: (1) diffuse-porous hardwoods, in which numerous and barely visible or invisible pores are evenly distributed throughout the growth ring (silver maple) or decrease gradually in size from earlywood to latewood, sometimes appearing as semi-ring porous (hybrid poplar and aspen); and (2) ring-porous hardwoods, in which earlywood pores ($>$100 μm) are much larger than latewood pores (abrupt transition) (oak and white ash).

The impregnation formulation was made from a hydroquinone-inhibited monomer [MMA: $H_2C = C(CH_3)COOCH_3$; Univar Canada, Richmond, BC, Canada], mixed with 0.5 wt% of Vazo 52 [2,2′-azobis-2,4-dimethylvaleronitrile, $(CH_3)_2C(CN)N = NC(CH_3)_2(CN)$], a low-temperature polymerization initiator purchased from DuPont Canada (Mississauga, Ontario, Canada). The 0.5 wt% of Vazo 52 was based on the weight of the mixture with polymeric monomer.

Preparation of hardened wood

All wood specimens (different size with thickness of 25 mm) from the six species were placed in a conditioning room for 1 week to reach 9% moisture content before impregnation. Specimens were then weighed and placed in an impregnation autoclave, then pressure vacuumed at below 75 mmHg for 20 min. Next, the impregnation solution was introduced into the autoclave to immerse the wood samples. A pressure of 1.38 MPa (200 psi) was applied to the autoclave and room temperature was maintained for 20 min to ensure maximum impregnation. After pressure release, impregnated samples were removed from the autoclave and excess monomer was wiped from the surface. Specimens were weighed and placed in the reactor for polymerization at 690 kPa (100 psi) nitrogen pressure and cured for 4 h at 70°C. After curing, the reactor was depressurized and samples were removed and placed in a ventilated area to allow the non-polymerized monomer to evaporate. Excess polymer was removed from the surface of some samples. Composite weights were measured again in the final samples with all samples weighed to the nearest 0.01 g. Polymer impregnation (PI) and retention (PR) in the composites were calculated according to the following equation:

$$IR(\%) = (w_{IW} - w_S)/w_S \times 100 \quad (2)$$

where w_{IW} and w_{HS} are the weights of impregnated and hardened wood samples and w_S is the initial weight of the corresponding solid wood sample.

To evaluate the effects of the impregnation process on wood porosity, MIP tests were conducted on both solid and hardened wood samples to compare results before and after hardening. Three or four specimens (depending on availability) of each wood species were machined from the same hardened pieces used for the MIP test. To maintain porosimeter accuracy, MIP test samples were machined into pieces 9 mm long with transverse sections of 8×8 mm.

Mercury intrusion porosimetry

Porosimetry was determined using Micrometrics AutoPore III 9420, which allows high pressure up to 414 MPa (60,000 psi), theoretically corresponding to a pore diameter of 3 nm. Surface tension was set at 0.485 Nm^{-1} and contact angle was set at 130° (advancing and receding), for the calculation of pore size distribution.

For the MIP tests, samples were first oven-dried at 103 ± 2°C for 24 h to remove the moisture contained in the pores. Samples were then weighed and placed in a penetrometer, which consists of a sample cup with a metal cap. The assembly was then sealed and placed in a low-pressure port, where the sample was evacuated at < 50 μmHg for 5 min to remove air and moisture. The sample cup was then filled with mercury to surround the specimen, and pressure was gradually raised to 207 kPa (30 psi) (low-pressure run), with equilibration time at 10 s. The assembly was then placed in a high-pressure port, with pressure up to 414 MPa and an automatic equilibration time of 10 s. Pore diameter, mean diameter, and cumulative and incremental intruded volume were recorded with corresponding pressures by micrometrics AutoPore III 9420 at approximately 58 points for each sample during total testing.

Results and discussion

Porosity and cell-wall density

MIP test results on solid wood and corresponding hardened wood samples are presented in Table I. Bulk density increased by 45–130% after treatment, depending on species. Compared to solid wood, total porosities of hardened wood specimens measured by MIP are dramatically lower, ranging from 35% for oak to 65% for aspen. This may be attributed to the PMMA polymer-filled void space within the wood. The polymer either blocked the channels through which mercury was injected into the pores or occupied the overall lumina. In previous studies, the enhancement of dimensional stability of wood–MMA composites was also attributed to this phenomenon (Elvy et al., 1995; El-Awady, 1999; Zhang et al., 2006). Porosities of impregnated samples ranged from 21.1% to 40.7%. The values found in this study are relatively high, indicating the presence of unfilled voids within the wood samples. This could be explained by several factors, such as evaporation during weight measurement and curing, incomplete impregnation during treatment, gaps at the cell wall–polymer interface after polymerization due to high vapour pressure of the MMA (Zhang et al., 2006), or MMA shrinkage after polymerization, causing small void spaces (Ibach & Ellis, 2005).

The skeletal densities of solid wood for the six species in Table I ranged from 1062 to 1375 kg m^{-3}, and these values are lower than those for cell fibre walls (which in general can be estimated to be about 1500 kg m^{-3}), as well as values reported in previous studies (Stayton & Hart, 1965; Moura et al., 2005; Almeida & Hernández, 2007). These differences could be explained by the presence of extractives in the wood samples, which would lower their densities (Stamm, 1929), and differences in the sample specifications. Almeida and Hernández (2007) used MIP to measure the cell-wall densities of 3 mm long samples of seven hardwood species and obtained values ranging from 1300 to 1438 kg m^{-3}. Higher cell-wall densities (1440–1445 kg m^{-3}) were measured on 320 μm thick wood samples of three softwoods using MIP (Stayton & Hart, 1965). Moura et al. (2005) reported 1290 kg m^{-3} as the skeletal density for one softwood (*Pinus sylvestris*) and 1430 and 1450 kg m^{-3} for two hardwoods (*Eucalyptus globulus* and *Betula verrucosa*), without specifying sample size. However, after measuring cell-wall density with other methods, such as helium gas displacement or pycnometry with different liquids, Stamm (1929) reported that wood cell-wall density ranged from 1466 to 1548 kg m^{-3} for both hardwoods and softwoods. The lower wood densities in the present study suggest incomplete mercury penetration due to thicker samples and/or certain amounts of isolated voids. Schneider (1983) reported that when the axial length of wood specimens used for MIP is several times greater than the fibre or tracheid length, the microvoids will only be filled when penetration pressures are sufficiently high to drive the mercury through the pits. The cause of the enclosed voids in the current study was attributed to the drying method and compression effect under high pressure, as mentioned above. It was reported that wood pore volume shifted from 0.002 $cm^3\ g^{-1}$ for oven-dried samples to 0.015 $cm^3\ g^{-1}$ for solvent-exchange-dried samples, using the nitrogen adsorption technique (Papadopoulos et al., 2003). It also seems that the ink-bottle effect becomes more apparent with increasing axial length of the specimen. Accordingly, total porosity values of the

Table I. Results of mercury intrusion porosimetry (MIP) for solid and hardened wood samples of six species, previous values of some species and polymer retention.

	Solid wood				Hardened wood			
	Porosity	Bulk density	Skeletal density (kg m^{-3})[b]		Porosity	Bulk density	Impregnation rate	Polymer retention
Wood species	(%)	(kg m^{-3})[a]	Present	Historical	(%)	(kg m^{-3})	(%)	(%)
White ash	49.4±1.2	695±11	1375±50	–	27.4±6.7	1026±20	47±4	46±5
Aspen	60.0±2.3	425±3	1062±62	–	21.1±3.4	982±85	134±2	115±7
White cedar	68.0±1.7	356±12	1116±95	1445–1548[c]	37.3±2.5	808±26	167±3	144±3
Silver maple	52.0±1.9	623±45	1298±72	–	26.6±7.5	975±121	57±13	56±13
Red oak	55.4±2.1	596±71	1332±99	1473–1540[d]	36.1±3.49	862±42	50±8	36±3
Hybrid poplar	70.6±1.4	340±30	1154±59	1020–1200[e]	40.7±7.1	770±64	183±13	164±14

Note: data are shown as mean±SD.
[a] Bulk density is based on anhydrous mass and volume, determined by MIP test at 0.004 MPa; [b] skeletal density determined by MIP at 414 MPa; cited from [c] Stamm (1929) and Stayton and Hart (1965), [d] Stamm (1929) and [e] Jayme and Krause (1963).

investigated species are expected to be somewhat lower than theoretical values.

Pore size distribution

Typical MIP curves for incremental and cumulative intruded volume versus pore diameter for solid wood are presented in Figure 2. This typical pattern was obtained for all the species studied. A second intrusion test was conducted on the same sample for comparison purposes. Both incremental and cumulative porosity values in the second time intrusion test were significantly lower. This indicates that most of the intruded mercury was trapped within the samples after the first intrusion. This hysteresis could be attributed to either the ink-bottle effect (Figure 1b, d), which is in good agreement with previous studies (Trenard, 1980; Schneider, 1983; Almeida & Hernández, 2007) and/or the difference between advancing and receding contact angles (Almeida & Hernández, 2007). This confirms the poor mercury penetration for the 9 mm long samples, even under very high pressure (414 MPa). Further, most of the detected second intrusion volume (>75%) was in pores with a diameter greater than 0.1 μm. The distribution of the second time incremental intrusion volume for the studied species is presented in Table II. The large amount of mercury found in pore diameters smaller than 0.1 μm also reflects the complexity and interconnectivity of wood microvoids (e.g. fibres and vessels). In addition, total porosities for all species in the second intrusion were not negligible.

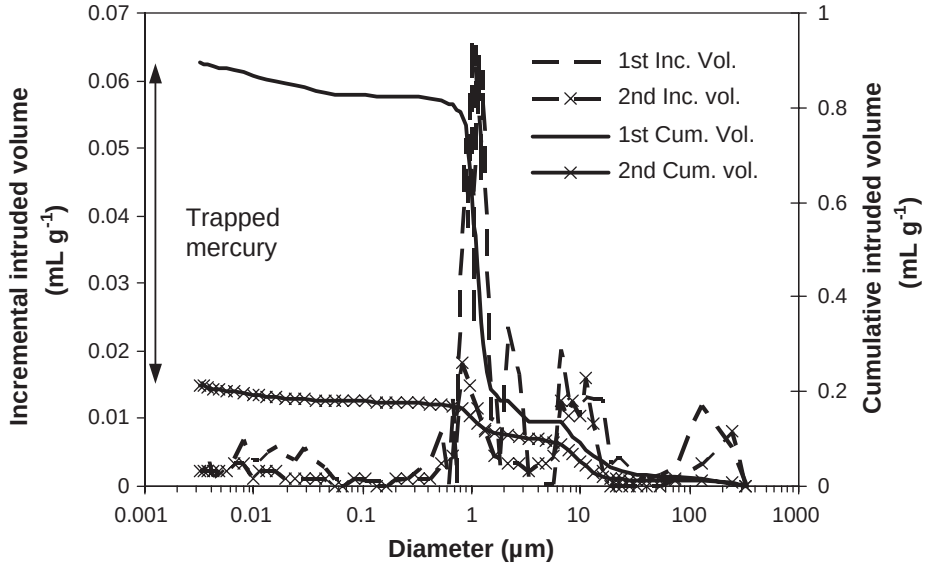

Figure 2. Typical curves for incremental and cumulative intruded volume versus pore diameter. Solid line = first intrusion curves; marked line = second intrusion curves.

Table II. Distribution of second incremental intruded volume (ml g^{-1}) and porosity (%) for solid wood samples of six species.

Diameter (μm)	White ash	Red oak	Silver maple	E. white cedar	Aspen	Hybrid poplar
$d > 3$	0.0434	0.1046	0.1022	0.0609	0.1328	0.2184
$0.1 < d \leq 3$	0.0621	0.1106	0.0769	0.0662	0.0443	0.1847
$d \leq 0.1$	0.0352	0.0564	0.0345	0.0318	0.0322	0.0255
Total volume (ml g^{-1})	0.1407	0.2716	0.2136	0.1590	0.2093	0.4286
Total porosity (%)	9.81	15.13	12.67	5.73	8.93	14.82

The typical incremental intrusion volume (ml g^{-1}) curves versus pore diameter (μm) for both solid wood and hardened wood (Figure 3) display three distinctive regions according to pore diameter: $d > 3$ μm, 0.1 μm $< d \leq 3$ μm, and $d \leq 0.1$ μm. MMA impregnation substantially changed the distribution of incremental intrusion volume compared to that of solid wood. Average incremental intrusions for the six studied species are presented in Figure 4. The repetition tests for both solid and hardened wood for each species show very similar intrusion volume and pore diameter distributions. This suggests that pore structure and porosity are intrinsic properties of each wood species. This finding is valid for similar-sized specimens only.

Table III presents the distribution of incremental intrusion volume in the three size regions for the six species. The pore volume available for mercury intrusion was much lower in all hardened wood samples. Total available volume by mercury was much lower, ranging from 55.67% for oak to 84.60% for aspen. This reduction is attributed to the significant decrease in pore volume available for mercury in pore diameter regions 1 and 2 after hardening, where decreased rates of 52.3% (cedar) to 91.1% (aspen) and 88.5% (oak) to 95.0% (aspen) were observed. Of the initial assumptions, intrusion volume was found to be increased only in pore region 3, ranging from 16.7% (oak) to a very high value of 1025.8% (hybrid poplar).

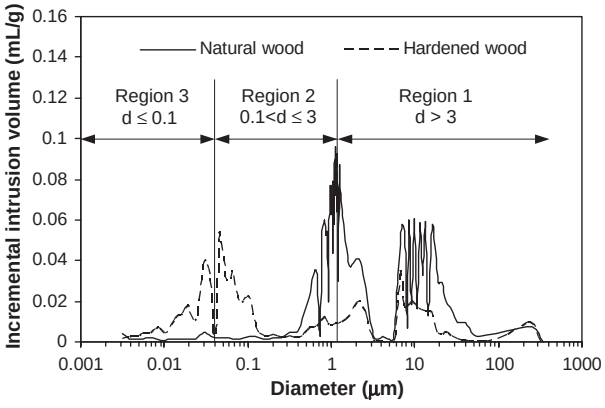

Figure 3. Typical curves for incremental intrusion volume versus pore diameter for natural and hardened wood samples.

Overall, it seems that the decreased rate was more uniform (around 90%) in pore diameter region 2 than in the other two regions. This might be due to the small amount of evaporation or retraction once the monomer entered the fibre lumina through the pits, even when the ambient pressure was at atmospheric pressure, with the pits acting as bottlenecks. Furthermore, most of the intrusion mercury volume in solid wood was found in region 2, with the least found in region 3. However, in hardened wood, most intruded volume was found in region 3, followed by region 2, except for oak. Therefore, MMA successfully penetrated the larger pores (diameter > 0.1 μm) in all species. It appears that the shift in pore volume distribution is mainly attributable to the chemical impregnation. As for the hardened oak wood, a ring-porous species, the shift in pore volume distribution can be explained by the relatively large proportion of pore volume with diameter greater than 3 μm. In addition, more monomer leaked after impregnation in oak than in other woods, as shown in the porosity values in Table I. For white cedar, aspen, and hybrid poplar, peaks are observed in region 3 after treatment, whereas no or only minor peaks are seen beforehand. This difference in intrusion volume is probably caused by the diffusion of MMA polymer within the wood.

MIP is also useful in identifying natural microstructural features of wood species, albeit indirectly (Stayton & Hart, 1965; Schneider & Wagner, 1974; Schneider, 1979; Persenaire et al., 2004; Grioui et al., 2007). The highest peak regions are found in pore diameters from 0.1 to 3 μm in all species, although values differ. One or two other peaks may occur, depending on species. In general, mercury penetrates into elements having pore diameters from 6 to 340 μm, which corresponds to the diameters of vessels, rays and open cutting fibres in hardwoods, and the diameters of tracheid and ray cells in softwood. The secondary pathway, ranging from 0.1 to 3 μm, may reflect the size of longitudinal and radial perforations in the fibres and vessels. The last pore region that mercury can reach has diameters below 0.1 μm, or cell-wall micropores. For

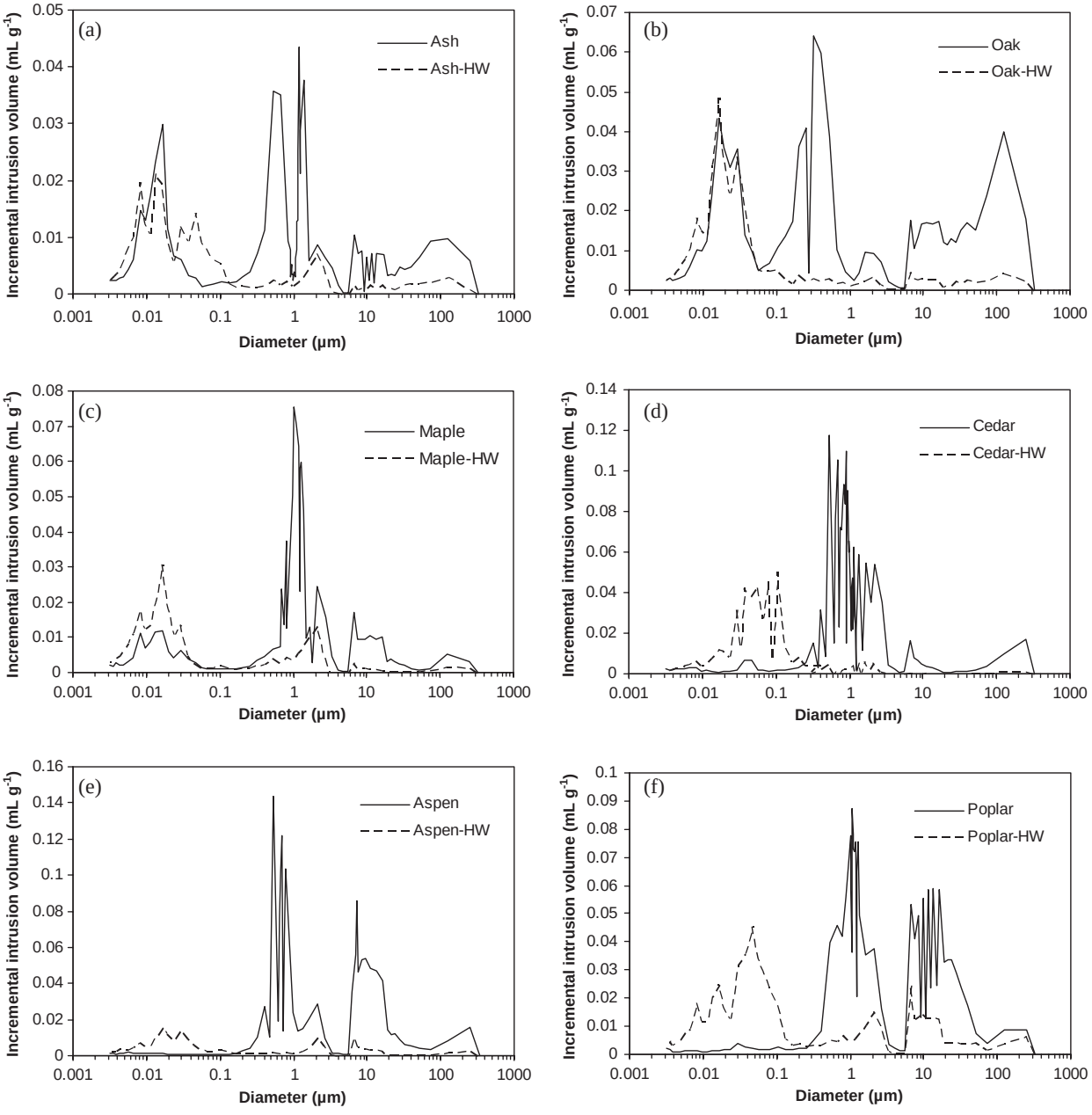

Figure 4. Average mercury intrusion porosimetry (MIP) incremental intrusion volume versus pore diameter curves for natural and hardened wood (HW) samples of six species.

instance, as reported in the literature (Bendtsen et al., 1981; Mátyás & Peszlen, 1997), vessel diameter and fibre lumen diameters in hybrid poplar ranged from 76 to 131 μm and 15 to 28 μm, respectively. Persenaire et al. (2004) reported two separate pore size distributions of 8–40 μm and 0.5–1 μm, and a rapid intrusion volume increase was also found in the MIP graph for poplar wood, with similar patterns in these distributions to those in the present study. However, in this study, MIP was unable to determine the proportion of different cell components in this study owing to the shift in pore volume caused by the ink-bottle effect.

Relationships between impregnation rate, polymer retention and wood porosity

The relationships between porosity and impregnation rate, and porosity and polymer retention are shown in Figure 5(a–d), respectively. When total raw porosity is used in the regressions, high correlations (R^2 of 0.92 and 0.89) are obtained (Figure 5a, c). From the above discussion, it is doubtful whether MMA penetrated into small pores with diameter $d < 0.1$ μm. However, many authors (Meyer, 1981; Schneider, 1994; Ibach & Ellis, 2005) suggest that vinyl monomer (MMA) occupies only the cell cavities, and not the cell wall.

Table III. Distribution of incremental intrusion volume (ml g^{-1}) for solid and hardened wood samples for six species.

	Diameter (μm)							
	$d>3$	$0.1<d\leq3$	$d\leq0.1$	Total	$d>3$	$0.1<d\leq3$	$d\leq0.1$	Total
Species	Solid wood				Hardened wood			
White ash	0.124±0.024	0.430±0.017	0.157±0.050	0.710±0.011	0.026±0.009	0.044±0.043	0.197±0.022	0.267±0.067
Red oak	0.306±0.075	0.368±0.083	0.268±0.022	0.942±0.160	0.063±0.021	0.042±0.020	0.313±0.049	0.418±0.066
Maple	0.108±0.060	0.638±0.104	0.094±0.029	0.840±0.080	0.017±0.010	0.070±0.025	0.195±0.08	0.282±0.111
Aspen	0.503±0.054	0.889±0.005	0.020±0.001	1.413±0.053	0.045±0.029	0.045±0.019	0.128±0.017	0.218±0.052
Hybrid poplar	0.584±0.097	1.499±0.032	0.032±0.016	2.115±0.215	0.150±0.046	0.111±0.057	0.361±0.080	0.622±0.161
Cedar	0.094±0.031	1.770±0.062	0.047±0.009	1.910±0.031	0.045±0.006	0.095±0.005	0.359±0.050	0.462±0.046

Note: data are shown as mean±SD.
[a] Mean represents the mean intruded volume (ml g^{-1}).

Thus, when porosity is corrected for pore diameter regions 1 and 2 ($d>0.1$ μm), higher correlations ($R^2=0.98$ for both) between impregnation rate, polymer retention and corrected porosity are observed (Figure 5b, d). This indicates that the porosity of the wood samples is the influencing factor on impregnation, especially for void spaces with pore diameter greater than 0.1 μm, potentially the threshold diameter for MMA monomer penetration.

Conclusions

Porosity characteristics were determined using MIP in solid and MMA-hardened wood samples of five hardwood and one softwood species. Both impregnation rate and polymer retention were highly correlated with wood porosity. Wood species with the highest porosities showed the highest impregnation rates and polymer retention. The porosities of MMA-hardened samples were noticeably lower than those for corresponding solid wood samples, the MMA impregnation solution having filled the wood voids, especially those with a diameter greater than 0.1 μm. The increased proportion of pores with a diameter less than 0.1 μm after impregnation supports this finding.

Acknowledgements

The authors are grateful to the Canada Research Chair Program, the Ministère de développement,

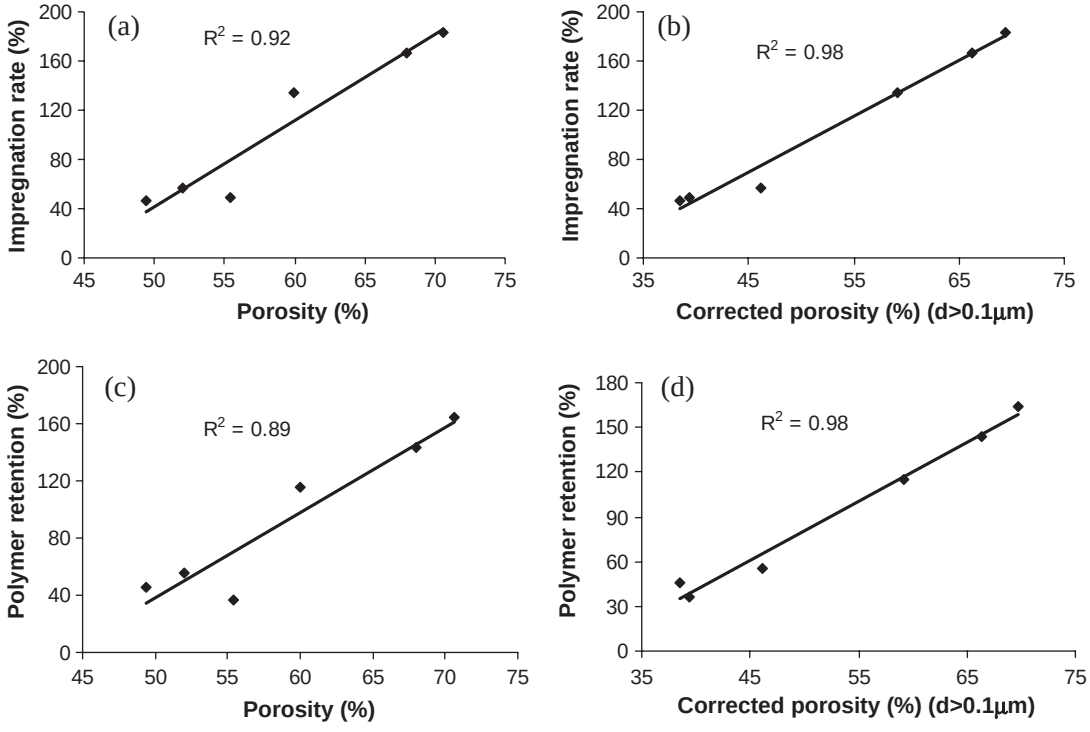

Figure 5. Correlations between porosity (%) and impregnation rate (%), and porosity (%) and polymer retention (%). (a, c) Porosity: total porosity of wood; (b, d) corrected porosity: porosity of wood with pore diameter $d>0.1$ μm.

de l'innovation et de l'exportation du Québec (MDEIE) and the NSERC-UQAT-UQAM Industrial Chair in Sustainable Forest Management for funding. The authors also acknowledge the assistance of Thomas Deschamps and Tommy Savoie (SEREX) for the MIP and wood hardening tests, respectively.

References

Almerida, G. & Hernández, R. (2007). Influence of the pore structure of wood on moisture desorption at high relative humidities. *Wood Material Science and Engineering*, *2*, 33–44.

Andersson, S. (2006). *A study of the nanostructure of the cell wall of the tracheids of conifer xylem by X-ray scattering*. PhD thesis, University of Helsinki [pdf].

Bendtsen, B. A., Maeglin, R. R. & Deneke, F. (1981). Comparison of mechanical and anatomical properties of eastern cottonwood and *Populus* hybrid NE-237. *Wood Science*, *14*(1), 1–14.

Cook, R. A. & Hover, K. C. (1993). Mercury porosimetry of cement-based materials and associated correction factors. *Construction and Building Materials*, *7*, 231–240.

Delage, P. & Lefebvre, G. (1984). Study of the structure of a sensitive Champlain clay and of its evolution during consolidation. *Canadian Geotechnical Journal*, *21*, 21–35.

El-Awady, N. I. (1999). Wood polymer composites using thermal and radiation techniques. *Journal of Reinforced Plastics and Composites*, *18*, 1367–1374.

Elvy, S. B., Dennis, G. R. & Ng, L. T. (1995). Effects of coupling agent on the physical properties of Wood–polymer composites. *Journal of Materials Processing Technology*, *48*, 365–372.

Forsström J. (2004). *Fundamental aspects on the re-use of wood based fibres—Porous structure of fibres and ink detachment.* PhD thesis. Trita-FPT Report 2004:37.

Grioui, N., Halouani, K., Zoulalian, A. & Halouani, F. (2007). Experimental study of thermal effect on olive wood porous structure during carbonization. *Maderas: Ciencia y Tecnologia*, *9*(1), 15–28.

Hill, C. A. S. & Papadopoulos, A. N. (2001). A review of methods to determine the size of the cell wall microvoids of wood. *Journal of the Institute of Wood Science*, *15*, 337–345.

Ibach, R. E. & Ellis, W. D. (2005). Lumen modifications. *In*: R. M. Rowell (ed.) Handbook of Wood Chemistry, New York: CRC Press, 421–446.

Jakob, H. F., Tschegg, S. E. & Fratzl, P. (1996). Hydration dependence of the wood-cell wall structure in *Picea abies*. A small-angle X-ray scattering study. *Macromolecules*, *29*, 8435–8440.

Jayme, G. & Krause, T. (1963). On the packing density of the cell walls in deciduous woods. *Holz als Roh- und Werkstoff*, *21*, 14–19.

Mátyás, C. & Peszlen, I. (1997). Effect of age on selected wood quality traits of poplar clones. *Silvae Genetica*, *46*, 64–72.

Meyer, J. A. (1981). Wood–polymer materials: State of the art. *Wood Science*, *14*(2), 49–54.

Moura, M. J., Ferreira, P. J. & Figueiredo, M. M. (2005). Mercury intrusion porosity in pulp and paper technology. *Power Technology*, *160*, 61–66.

Ona, T., Sonoda, T., Ito, K., Shibata, M., Ootake, Y., Ohshima, J., et al. (1999). In situ determination of proportion of cell types in wood by Fourier transform raman spectroscopy. *Analytical Biochemistry*, *268*, 43–48.

Papadopoulos, A. N., Hill, C. A. S. & Gkaraveli, A. (2003). Determination of surface area and pore volume of holocellulose and chemically modified wood flour using the nitrogen adsorption technique. *Holz als Roh- und Werkstoff*, *61*, 453–456.

Penumadu, D. & Dean, J. (2000). Compressibility effect in evaluating the pore-size distribution of kaolin clay using mercury intrusion porosimetry. *Canadian Geotechnical Journal*, *37*, 393–405.

Persenaire, O., Alexandre, M., Degeé, P., Pirard, R. & Dubois, P. (2004). End-grained wood–polyurethane composites, 1 synthesis, morphology and characterization. *Macromolecular Materials and Engineering*, *289*, 895–902.

Roels, S., Elsen, J., Carmeliet, J. & Hens, H. (2001). Characterisation of pore structure by combining mercury porosimetry and micrography. *Materials and Structures/Materiaux et Constructions*, *34*(236), 76–82.

Schneider, A. (1979). Analysis the porosity of wood with the mercury porosimeter. *Holz als Roh- und Werkstoff*, *41*, 295–302.

Schneider, A. (1983). Investigations on the suitability of mercury porosimetry for the evaluation of wood impregnability. *Holz als Roh- und Werkstoff*, *41*, 101–107.

Schneider, A. & Wagner, L. (1974). Determination of pore distribution in wood with a mercury porosimeter. *Holz als Roh- und Werkstoff*, *32*, 216–224.

Schneider, M. H. (1994). Wood polymer composites. *Wood and Fiber Science*, *26*, 142–151.

Solpan, D. & Güven, O. (1999a). Improvement of mechanical stability of beech wood by radiation-induced in situ copolymerization of allyl glycidyl ether with acrylonitrile and methyl methacrylate. *Journal of Applied Polymer Science*, *71*, 1515–1523.

Solpan, D. & Güven, O. (1999b). Preparation and properties of some wood/(co)polymer composites. *Die Angewande Makromolekulare Chemie*, *269*, 30–35.

Solpan, D. & Güven, O. (2000). A comparative study of using allyl alcohol based copolymers in the preservation of wood: oak vs. cedar. *Polymer Composites*, *21*, 196–201.

Solpan, D. & Güven, O. (2001). Modification of some mechanical properties of spruce by radiation induced copolymerization of acrylonitrile and methyl methacrylate with ally1 glycidyl ether. *Polymer Composites*, *22*, 90–96.

Stamm, A. J. (1929). Density of wood substance, adsorption by wood and permeability of wood. *Journal of Physical Chemistry*, *33*, 398–414.

Stayton, C. L. & Hart, C. A. (1965). Determining pore-size distribution in softwoods with a mercury porosimeter. *Forest Products Journal*, *15*, 435–440.

Stone, J. E. (1964). The porous structure of wood and fibers. *Pulp and Paper Magazine of Canada*, *65*(1), T3–T13.

Trenard, P. Y. (1980). Comparaison et interpretation de courbes obtenues par porosimétrie au mercure sur diverses essences de bois. *Holzforschung*, *34*, 139–146.

Wang, W. Q. & Yan, N. (2005). Characterizing liquid resin penetration in wood using a mercury intrusion porosimeter. *Wood and Fiber Science*, *37*, 505–513.

Washburn, E. W. (1921). Note on a method of determining the distribution of pore sizes in a porous material. *Proceedings, National Academy of Science*, *7*, 115–116.

Zhang, Y. L., Zhang, S. Y., Yang, D. Q. & Wan, H. (2006). Dimensional Stability of Wood–Polymer Composites. *Journal of Applied Polymer Science*, *102*, 5085–5094.